

Nodal domains on isospectral quantum graphs: the resolution of isospectrality?

Ram Band¹, Talia Shapira¹ and Uzy Smilansky^{1,2}

¹ Department of Physics of Complex Systems, The Weizmann Institute of Science, Rehovot 76100, Israel

² School of Mathematics, Bristol University, Bristol BS83EQ, UK

Received 12 July 2006, in final form 20 September 2006

Published 24 October 2006

Online at stacks.iop.org/JPhysA/39/13999

Abstract

We present and discuss isospectral quantum graphs which are not isometric. These graphs are the analogues of the isospectral domains in \mathbb{R}^2 which were introduced recently in Gordon *et al* (1992 *Bull. Am. Math. Soc.* **27** 134–8), Chapman (1995 *Am. Math. Mon.* **102** 124), Buser *et al* (1994 *Int. Math. Res. Not.* **9** 391–400), Okada and Shudo (2001 *J. Phys. A: Math. Gen.* **34** 5911–22), Jakobson *et al* (2006 *J. Comput. Appl. Math.* **194** 141–55) and Levitin *et al* (2006 *J. Phys. A: Math. Gen.* **39** 2073–82)) all based on Sunada's construction of isospectral domains (Sunada T 1985 *Ann. Math.* **121** 196–86). After presenting some of the properties of these graphs, we discuss a few examples which support the conjecture that by counting the nodal domains of the corresponding eigenfunctions one can resolve the isospectral ambiguity.

PACS numbers: 05.45.Mt, 02.30.Zz, 02.70.Hm

1. Introduction

M Kac's classical paper 'Can one hear the shape of a drum' [7] triggered intensive research in two complementary aspects of this problem. On the one hand, a search for systems for which Kac's question is answered in the affirmative was conducted, and, on the other hand, various examples of pairs of systems which are isospectral but not isometric were identified. In the present paper we shall focus our attention to quantum graphs and in the following lines will review the subject of isospectrality in this limited context. The interested reader is referred to [1–11] for a broader view of the field where spectral inversion and its uniqueness are discussed.

Spectral problems related to graphs emerge in two distinct ways. In the first, the spectrum of the connectivity (adjacency) matrix is considered. It represents a discrete version of the Laplacian, and for finite graphs, the spectrum is finite. This set of problems is often referred to as combinatorial graphs. Quantum (metric) graphs are obtained by associating the standard metric to the bonds which connect the vertices. The Schrödinger operator consists of the one-dimensional Laplacians on the bonds complemented by appropriate boundary conditions at

the vertices (see next section). The spectrum of quantum graphs is unbounded, and it displays many interesting features which made it a convenient paradigm in the study of quantum chaos [19].

Shortly after the appearance of Kac's paper, M E Fisher published his work 'On hearing the shape of a drum' [12], where he addresses isospectrality for the discrete version of the Laplacian. Since then, the study of isospectral combinatorial graphs made very impressive progress. In particular, several methods to construct isospectral yet different graphs were proposed. A review of this problem can be found in [14]. In particular, a method which was originally put forward by Sunada [6] to construct isospectral Laplace–Beltrami operators on Riemann manifolds was adapted for the corresponding problem in the context of combinatorial graphs. Here we shall go one step further, and show that it can be also adapted for quantum graphs.

The conditions under which the spectral inversion of quantum graphs is unique were studied previously. In [15, 16] it was shown that in general, the spectrum does not determine uniquely the length of the bonds and their connectivity. However, it was shown in [13] that quantum graphs whose bond lengths are *rationaly independent* 'can be heard'—that is—their spectra determine uniquely their connectivity matrices and their bond lengths. This fact follows from the existence of an exact trace formula for quantum graphs [18, 19]. Thus, isospectral pairs of non-congruent graphs must have rationally dependent bond lengths. The Sunada method, which is based on constructing the isospectral domains by concatenating several copies of a given building block, automatically provides us with graphs with rationally dependent lengths. An example of a pair of metrically distinct graphs which share the same spectrum was already discussed in [13]. In a previous report we have shown that all the known isospectral domains in \mathbb{R}^2 [3, 4] have corresponding isospectral pairs of quantum graphs [21]. Here, we shall take the subject one step further, and propose that isospectral graphs can be resolved by counting their nodal domains. That is, the nodal counts of eigenfunctions belonging to the same spectral value are not the same. The idea that nodal counts resolve isospectrality was suggested in [20] for a family of isospectral flat tori in 4D, and was tested numerically. The present work offers both rigorous and numerical evidence to substantiate the validity of this conjecture in a few examples of isospectral graphs. For these examples the nodal counts differences occur on a substantial fraction of the spectrum.

The paper is organized in the following way. For the sake of completeness we shall give a short review of some elementary definitions and facts on quantum graphs. We shall then show how pairs of isospectral domains in \mathbb{R}^2 can be reduced to isospectral pairs of quantum graphs, and discuss their spectra and eigenfunctions. Finally, we shall study the nodal domains of these eigenfunctions and show that by counting nodal domains one can resolve the isospectral ambiguity of the graphs presented.

1.1. A short introduction to quantum graphs

We consider finite graphs consisting of V vertices connected by B bonds. The $V \times V$ connectivity matrix will be denoted by $C_{i,j}$: $C_{i,j} = r$ when the vertices i and j are connected by r bonds, and it vanishes otherwise. The group of bonds which emerge from the vertex i forms a 'star' which will be denoted by $S^{(i)}$. The *valency* v_i of a vertex is defined as the cardinality of the star $S^{(i)}$ and $v_i = \sum_j C_{i,j}$. Vertices with $v_i = 1$ belong to the graph *boundary*. The vertices with $v_i > 1$ belong to the graph *interior*. The bonds are endowed with the standard metric, and the coordinates along the bonds b are denoted by x_b . The length of the bonds will be denoted by L_b , and the total length of the graph is $\mathcal{L} = \sum_b L_b$.

The domain of the Schrödinger operator on the graph is the space of functions which belong to Sobolev space $H^2(b)$ on each bond b and at the vertices they are continuous and obey boundary conditions as is mentioned in (1). The operator is constructed in the following way. On the bonds, it is identified as the Laplacian in 1D $-\frac{d^2}{dx^2}$. It is supplemented by boundary conditions on the vertices which ensure that the resulting operator is self-adjoint. We shall consider in this paper the Neumann and Dirichlet boundary conditions:

$$\begin{aligned} \text{Neumann} \quad \forall i : \sum_{b \in S(i)} \frac{d}{dx_b} \psi_b(x_b) \Big|_{x_b=0} &= 0, \\ \text{Dirichlet} \quad \forall i : \psi_b(x_b)|_{x_b=0} &= 0. \end{aligned} \tag{1}$$

The derivatives in (1) are directed out of the vertex i . *Comment:* the Neumann boundary conditions will be assumed throughout, unless otherwise stated. A wavefunction with a wave number k can be written as

$$\psi_b(x_b) = \frac{1}{\sin k L_b} (\phi_i \sin k(L_b - x_b) + \phi_j \sin k x_b), \tag{2}$$

where b connects the vertices i and j , where the wavefunction ψ_b takes the values ϕ_i and ϕ_j , respectively. The form (2) ensures continuity. The spectrum $\{k_n\}$ and the corresponding eigenfunctions are determined by substituting (2) into (1). The resulting homogeneous linear equations for the ϕ_i are written as

$$\forall 1 \leq i \leq V : \sum_{j=1}^B A_{i,j}(L_1, \dots, L_B; k) \phi_j = 0, \tag{3}$$

and a non-trivial solution exists when

$$f(L_1, \dots, L_B; k) \doteq \det A(L_1, \dots, L_B; k) = 0. \tag{4}$$

The spectrum $\{k_n\}$, which is a discrete, positive and unbounded sequence is the zero set of the *secular function* $f(L_1, \dots, L_B; k)$. The secular functions of the type (4) have poles on the real k axis, which renders them rather inconvenient for numerical studies. The secular function can be easily regularized in various ways (see, e.g. [19, 21]).

It is easy to show that the complete wavefunction can be written down in terms of the vertex wavefunctions at the interior vertices with $v_i \geq 3$ only. In what follows we shall denote their number by V_{int} . This reduces the dimension of the matrix A above from V to V_{int} .

The nodal domains of the eigenfunctions (the connected domains where the wavefunction is of constant sign) are of two types. The ones that are confined to a single bond are rather trivial. Their length is exactly half a wavelength and their number is on average $\frac{kL}{\pi}$. The nodal domains which extend over several bonds emanating from a single vertex vary in length and their existence is the reason why counting nodal domains on graphs is not a trivial task. The number of nodal domains in a general graph can be written as

$$\nu_n = \frac{1}{2} \sum_i \sum_{b \in S(i)} \left\{ \left\lfloor \frac{k_n L_b}{\pi} \right\rfloor + \frac{1}{2} (1 - (-1)^{\lfloor \frac{k_n L_b}{\pi} \rfloor}) \text{sign}[\phi_i] \text{sign}[\phi_j] \right\} - B + V, \tag{5}$$

where $\lfloor x \rfloor$ stands for the largest integer which is smaller than x , and ϕ_i, ϕ_j are the values of the eigenfunction at the vertices connected by the bond b [22]. Equation (5) holds for the case of an eigenfunction which does not vanish on any vertex: $\forall i \phi_i \neq 0$.

Recently Schapotschnikow [23] proved that Sturm's oscillation theorem extends to finite tree (loop-less) graphs: the number of nodal domains of the n th eigenfunction (ordered by increasing eigenvalues) is n . Berkolaiko [24] have shown that the number of nodal domains

is bounded to the interval $[n - l, n]$ where l is the minimal number of bonds which should be cut so that the resulting graph is a tree.

Nodal domains can be also defined and counted in an alternative way which makes use of the vertex wavefunctions $\{\phi_i\}$ (see (2)) exclusively:

A nodal domain consists of a maximal set of connected interior vertices ($v_i \geq 3$) where the vertex wavefunctions have the same sign.

This definition has to be modified if any of the ϕ_i vanishes. Then, the sign attributed to it is chosen to maximize the number of nodal domains [25].

We thus have two independent ways to define and count nodal domains. To distinguish between them we shall refer to the first as *metric* nodal domains, and the number of metric domains in the n th eigenfunction will be denoted by v_n . Berkolaiko's theorem states that $(n - l) \leq v_n \leq n$. The domains defined in terms of the vertex wavefunctions will be referred to as the *discrete* nodal domains. The number of discrete nodal domains of the n th vertex wavefunction will be denoted by μ_n . The sequences of metric and discrete nodal domain counts $\{v_n\}$ and $\{\mu_n\}$ are the main objects of the study of the present paper.

2. Isospectral quantum graphs

The first pair of isospectral planar domains which was introduced by Gordon, Web and Wolpert [1] is a member of a much larger set which was discussed in [3, 4]. This was extended in [5] to include domains which differ in the distribution of boundary conditions (Dirichlet or Neumann) along their boundaries. The common feature of these sets of pairs of isospectral domains is that they are constructed using the Sunada method [6], and they share a few important and distinctive attributes:

- The domains are constructed by concatenating an elementary 'building block' in two different prescribed ways to form the two domains. A building block is joined to another by reflecting along the common boundary. The shape of the building block is constrained only by symmetry requirements, but otherwise it is quite general.
- The eigenfunctions corresponding to the same eigenvalue are related to each other by a *transplantation*. That is, the eigenfunction in a building block of one domain can be expressed as a linear combination of the eigenfunction in several building blocks in the other domain. The transplantation matrix is independent of the considered eigenvalue.
- The construction of these pairs reflects an abstract algebraic structure which was identified by Sunada [6].

An example of an isospectral pair of domains in \mathbb{R}^2 and its building block is given in figure 1(a). This is a pair whose construction is described in [3]. It is denoted there by 7_3 . Other examples are displayed in, e.g. [2, 3, 5].

We can construct *metric* graphs which are analogous to these domains, by replacing the building blocks by appropriate graphs which preserve the required symmetry. As an example, the triangular building block in figure 1(a) can be replaced by a three star with bonds of lengths a , b and c as shown in figure 1(b). This yields the pair of isospectral but non-isometric graphs shown in figure 1(c). (In drawing figure 1(c) we took advantage of the fact that the 'angles' between the bonds are insignificant). Note that the two graphs share the same connectivity matrix (they are topologically congruent) however they are not isometric. As a matter of fact the right and the left graphs are interchanged when the bonds ' b ' with ' c ' are switched. Thus, the lengths b and c must be different to ensure that the two graphs are not isometric. This is an example of an asymmetry requirement which the building block must satisfy. All other pairs

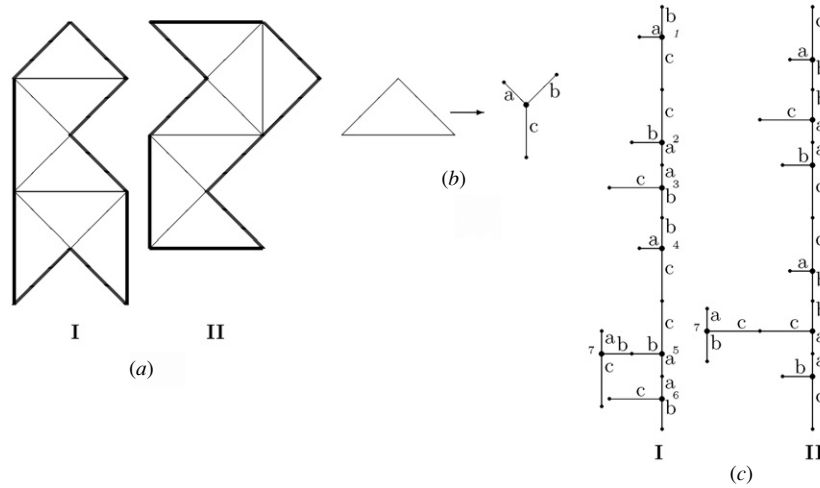


Figure 1. (a) Planar isospectral domains of the 7_3 type. (b) Reducing the building block to a three star. (c) The resulting isospectral quantum graphs.

of isospectral domains proposed in [3] can be converted to their analogous quantum graphs (see [21] for details). Two examples are shown in figure 2.

The simplest pair of isospectral domains can be built by applying the Sunada method to the Dihedral group D_4 . The resulting graphs are shown in figure 3, where the letters D or N specify the boundary conditions at the boundary vertices. (The boundary conditions at the interior vertices are always Neumann.) Note that the two graphs are connected differently, in contrast with the previous example where the topology of the two graphs is the same. In the appendix we give a brief description of the construction of this pair, as an example of the Sunada method.

In a way of illustration we shall write explicitly the secular functions for the graphs shown above. Starting with the 7_3 pair, we have $V_{\text{int}} = 7$ (the interior vertices are marked by a black dot and are enumerated in figure 1(c)). The secular function for the graph I is written in terms of the matrix

$$A(a, b, c; k) = \begin{pmatrix} \xi - \gamma & \gamma & 0 & 0 & 0 & 0 & 0 \\ \gamma & \xi - \alpha - \gamma & \alpha & 0 & 0 & 0 & 0 \\ 0 & \alpha & \xi - \alpha - \beta & \beta & 0 & 0 & 0 \\ 0 & 0 & \beta & \xi - \beta - \gamma & \gamma & 0 & 0 \\ 0 & 0 & 0 & \gamma & \xi - \alpha - \beta - \gamma & \alpha & \beta \\ 0 & 0 & 0 & 0 & \alpha & \xi - \alpha & 0 \\ 0 & 0 & 0 & 0 & \beta & 0 & \xi - \beta \end{pmatrix}. \tag{6}$$

Here,

$$\alpha(a; k) = \frac{1}{\sin(2ka)}, \quad \beta(b; k) = \frac{1}{\sin(2kb)}, \quad \gamma(c; k) = \frac{1}{\sin(2kc)} \tag{7}$$

and

$$\xi(a, b, c; k) = \tan(ak) + \tan(bk) + \tan(ck). \tag{8}$$

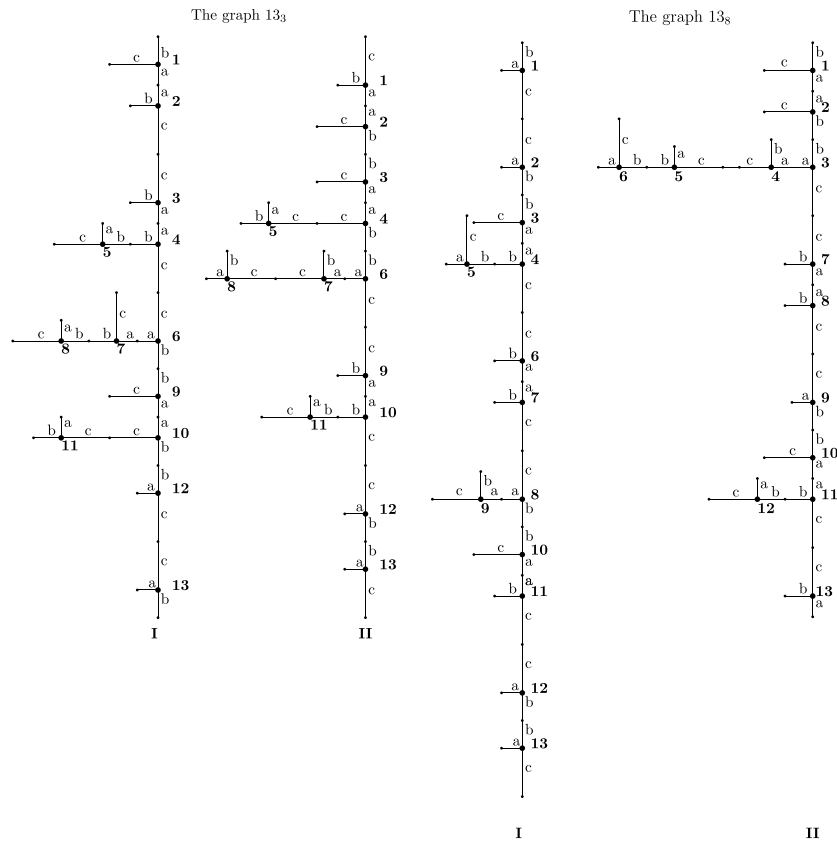


Figure 2. The isospectral pairs 13_3 (left) and 13_8 (right) [3].

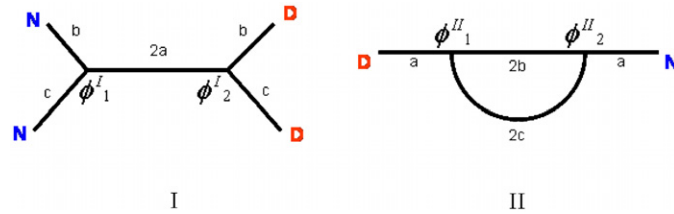


Figure 3. The isospectral pair with boundary conditions. D stands for Dirichlet and N for Neumann.

The corresponding vertex eigenfunction $\vec{\phi}^I = (\phi_1^I, \dots, \phi_7^I)$ is the eigenvector of $A(a, b, c; k_n)$ with a vanishing eigenvalue. The A matrix for the graph II is obtained from the matrix $A(a, c, b; k_n)$ by interchanging c and b . Explicit computation shows that $\det A(a, b, c; k) = \det A(a, c, b; k)$. This proves the isospectrality of the two graphs.

The sum of the elements of any of the columns of $A(a, b, c; k)$ is ξ . Hence the vector $\vec{1} = (1, 1, 1, 1, 1, 1, 1)$ is an eigenvector with an eigenvalue ξ . The values of k for which $\xi(a, b, c; k) = 0$ are in the spectrum of both graphs. They correspond to eigenfunctions which are the same on each of the three stars—the building block of the complete graphs

(figure 1(b)). As a matter of fact, the condition $\xi(a, b, c; k) = 0$ is the secular equation for this three star with bond lengths a, b, c [19]. This subset exhausts $1/7$ of the spectrum of the graphs, and in this set the transplation property is trivial.

The transplation property which is basic to the proof of isospectrality for the \mathbb{R}^2 domains in [3] can be explicitly formulated by the transplation matrix

$$T = \begin{pmatrix} 0 & 0 & 0 & 1 & 1 & 1 & 0 \\ 0 & 0 & 1 & 0 & 0 & 1 & 1 \\ 0 & 1 & 0 & 0 & 1 & 0 & 1 \\ 1 & 0 & 0 & 1 & 0 & 0 & 1 \\ 1 & 0 & 1 & 0 & 1 & 0 & 0 \\ 1 & 1 & 0 & 0 & 0 & 1 & 0 \\ 0 & 1 & 1 & 1 & 0 & 0 & 0 \end{pmatrix}, \quad \text{so that } \vec{\phi}^{\text{II}} = T\vec{\phi}^{\text{I}}. \quad (9)$$

We observe that the inverse transplation is also effected by T : $\vec{\phi}^{\text{I}} = T\vec{\phi}^{\text{II}}$, even though T is not self-inversive. The fact that T induces the transplation in the two directions implies that the vertex wavefunctions $\vec{\phi}$ must be eigenvectors of T^2 (as long as the eigenvalue is not degenerate). The wavefunctions are defined up to normalization, and therefore the corresponding eigenvalues can be different from unity. The spectrum of T^2 consists of the eigenvalue 9 and the six-fold degenerate eigenvalue 2. Thus, the vertex wavefunctions are either proportional to $\vec{1}$, or belong to the six-dimensional subspace of vectors orthogonal to $\vec{1}$. This observation will be used in the next section when the nodal structure of the eigenfunctions is to be discussed.

Other examples of pairs of isospectral graphs such as the pair described in [13] can be obtained from the isospectral graphs constructed above, by setting the length of the c bond to zero. This was explicitly shown in [21]. Using similar special cases one can generate a rich variety of isospectral but not isometric quantum graphs.

Finally, it should be emphasized, that the skeleton of interior vertices form graphs which are identical to the topological, coloured graphs which were introduced in [4] to express the transplation properties of the isospectral domains in \mathbb{R}^2 . The quantum, metric graphs can be obtained simply by completing each topological vertex to a three-vertex star graph with lengths a, b, c . Topological bonds are associated with lengths according to their colours, and bonds are added to the topological vertices with valency less than three, to complete them to three stars. This proves the statement made above that the computation carried out here can be repeated for any of the topological graphs shown in [4]. The graphs corresponding to the isospectral domains 13_3 and 13_8 are shown in figure 2.

The Dihedral graphs are much simpler, with $V_{\text{int}} = 2$. Their secular determinants can be shown to be identical functions of k . This is an explicit demonstration that the graphs are indeed isospectral. The secular equation is obtained from

$$A(a, b, c; k) = \begin{pmatrix} \eta - (\beta + \gamma) & -\alpha \\ -\alpha & \eta + (\beta + \gamma) \end{pmatrix}$$

$$\alpha(a; k) = \frac{1}{\sin(2ka)}, \quad \beta(b; k) = \frac{1}{\sin(2kb)}, \quad \gamma(c; k) = \frac{1}{\sin(2kc)} \quad (10)$$

$$\eta(a, b, c; k) = \cot(2ka) + \cot(2kb) + \cot(2kc).$$

As can be easily seen, $\det A$ has poles, and to get a regular secular function we have to multiply it by $\sin(2ka) \sin(2kb) \sin(2kc)$. It takes the form

$$f(a, b, c; k) = \sin(2ka)(-2 + 2 \cos(2kb) \cos(2kc) - 3 \sin(2kb) \sin(2kc)) + 2 \cos(2ka) \sin(2kb + 2kc). \quad (11)$$

The transplantation matrix for this pair of graphs is derived in the appendix. It reads

$$T = \frac{1}{\sqrt{2}} \begin{pmatrix} 1 & -1 \\ 1 & 1 \end{pmatrix}, \quad \text{so that } \vec{\phi}^{\text{II}} = T\vec{\phi}^{\text{I}}. \quad (12)$$

The eigenvectors $\vec{\phi}^{\text{I,II}}$ point at the directions $\theta^{\text{I,II}}$, with $\tan(\theta^{\text{I,II}}) = \frac{\phi_2^{\text{I,II}}}{\phi_1^{\text{I,II}}}$. The transplantation (12) implies that $\vec{\phi}^{\text{II}}$ is obtained from $\vec{\phi}^{\text{I}}$ by a rotation of $\frac{\pi}{4}$ counterclockwise. Direct substitutions shows that

$$\tan(\theta^{\text{I}}(k_n)) = g(a, b, c; k_n), \quad (13)$$

where

$$g(a, b, c; k) = \cos(2ka) + \sin(2ka) \left(\frac{\cos(2kb) - 1}{\sin(2kb)} + \frac{\cos(2kc) - 1}{\sin(2kc)} \right). \quad (14)$$

The explicit form of the functions $f(a, b, c; k)$ and $g(a, b, c; k)$ will be used in the discussion of nodal counting in the next section.

3. Nodal counts and the resolution of isospectrality

The real eigenfunctions of Laplace–Beltrami operators on two-dimensional manifolds display usually an intricate sets of nodal domains—which are the connected domains where the sign of the eigenfunction is constant [27]. Sturm’s oscillation theorem for systems in 1D, and its extension by Courant to any dimension, establishes the connection between the number of nodal domains and the spectrum: the number of nodal domains ν_n of the n th eigenfunction is bounded by n . (the eigenfunctions are arranged by increasing value of their eigenvalues). Courant’s theorem for combinatorial graphs and for quantum graphs were proved in [22, 25], respectively.

Given a pair of isospectral domains. Are the sequences of nodal counts $\{\nu_n\}_{n=1}^{\infty}$ identical? In other words, can one use the information stored in the nodal sequences to resolve isospectrality? This question was recently discussed in the context of isospectral flat tori in \mathbb{R}^d with $d \geq 4$ [20], and numerical as well as analytical evidence was brought to substantiate the conjecture that the nodal sequences resolve isospectrality. In this section we shall provide rigorous as well as numerical evidence to show that the same is true for isospectral quantum graphs of the types discussed above. We shall start by discussing the *discrete* nodal sequences and then proceed to the *metric* nodal sequences.

3.1. The discrete nodal sequences

The *discrete* nodal domains were defined as the maximally connected sets of interior vertices with vertex wavefunctions of equal sign. Their number is denoted by μ_n , and the nodal sequence is $\{\mu_n\}_{n=1}^{\infty}$. We shall prove in the next subsection that for the dihedral graphs half of the entries in the sequences of discrete nodal counts are different. We are not able to provide a similar proof for the more complex graphs, but we shall bring numerical evidence which supports the conjecture that their sequences of discrete nodal counts are different.

3.1.1. The dihedral graphs. The number of discrete nodal domains for this pair of dihedral graphs (see figure 3) can be either one or two, depending on whether the signs of the components of the (two dimensional) vertex eigenfunctions have the same sign or not. In other words (see (13)), the number of nodal domains depend on the quadrant in the (ϕ_1, ϕ_2) plane where the

eigenvectors point: $\mu = 1$ in the first and the third quadrants, and $\mu = 2$ in the second and the fourth quadrants:

$$\mu_n = 1 + \frac{1}{2}(1 - \text{sign}(\tan \theta_n)). \tag{15}$$

The transplantation implies that the eigenvectors $\vec{\phi}_n^{\text{II}}$ are obtained by rotating $\vec{\phi}_n^{\text{I}}$ by $\frac{\pi}{4}$ counterclockwise. Therefore, $\mu_n^{\text{I}} \neq \mu_n^{\text{II}}$ if the transplantation rotates the vectors across the quadrant borders. In other words,

$$\mu_n^{\text{I}} \neq \mu_n^{\text{II}} \iff \tan(\theta_n) \in \{(-1, 0) \cup (1, \infty)\}. \tag{16}$$

This observation is essential to our discussion since it expresses the problem of nodal counting in geometrical terms.

It is convenient to construct finite subsequences $\{\mu_n^{\text{I}}\}$ and $\{\mu_n^{\text{II}}\}$ of discrete nodal count of graphs I and II, restricted to the spectral points in the interval $0 \leq k_n \leq K$. We denote the number of terms by $N(K)$. Define

$$P(K) = \frac{1}{N(K)} \#\{n \leq N(K) : \mu_n^{\text{I}} \neq \mu_n^{\text{II}}\}. \tag{17}$$

We shall now prove the following theorem.

Theorem 1. *Consider the dihedral graphs I, II discussed above with rationally independent bond lengths a, b, c . Then*

$$\lim_{K \rightarrow \infty} P(K) = \frac{1}{2}. \tag{18}$$

Proof of theorem 1. The rational independence of a, b, c implies that the eigenfunctions never vanish on the inner vertices and hence that the spectrum is simple.

In order to study $P(K)$ above, we consider the distribution of the directions of the eigenfunctions $\vec{\phi}_n^{\text{I}}$ in the spectral interval. Using ((11), (13), (14)) we get

$$h(x; K) = \langle \delta(x - \tan \theta_n) \rangle_K = \frac{1}{N(K)} \int_0^K dk \delta(f(a, b, c; k)) \left| \frac{df}{dk} \right| \delta(x - g(a, b, c; k)). \tag{19}$$

In taking the limit $K \rightarrow \infty$ we use $N(K) = \frac{2a+2b+2c}{\pi} K$ [19]. Moreover, since a, b, c are assumed to be rationally independent, k creates an ergodic flow on the 3-torus T_3 spanned by $r = 2ka \text{ mod } 2\pi, s = 2kb \text{ mod } 2\pi, t = 2kc \text{ mod } 2\pi$ [26]. Ergodicity implies that the integral over k in (19) may be replaced by an integral over T_3 leading to

$$\begin{aligned} h(x) &= \frac{\pi}{2(a+b+c)} \frac{1}{\pi^3} \int_0^{2\pi} dr \int_0^{2\pi} ds \int_0^{2\pi} dt \delta(f(r, s, t)) \left| \frac{df}{dk} \right| \delta(x - g(r, s, t)) \\ &= \frac{1}{2(a+b+c)\pi^2} \int_0^{2\pi} ds \int_0^{2\pi} dt \left(\int_0^\pi dr \delta(f(r, s, t)) \left| \frac{df}{dk} \right| \delta(x - g(r, s, t)) \right. \\ &\quad \left. + \int_\pi^{2\pi} dr \delta(f(r, s, t)) \left| \frac{df}{dk} \right| \delta(x - g(r, s, t)) \right) \\ &= \frac{1}{2(a+b+c)\pi^2} \int_0^{2\pi} ds \int_0^{2\pi} dt [I_1(s, t; x) + I_2(s, t; x)]. \end{aligned} \tag{20}$$

Now we note that under the transformation $r \mapsto r' = (r + \pi) \text{ mod } 2\pi$ we have

$$\begin{aligned} f(r', s, t) &= -f(r, s, t) \\ \frac{df}{dk}(r', s, t) &= -\frac{df}{dk}(r, s, t) \\ g(r', s, t) &= -g(r, s, t). \end{aligned}$$

Thus, we conclude that

$$\begin{aligned}
 I_1(s, t; x) = I_2(s, t; -x) &\Rightarrow h(x) = h(-x) \\
 &\Rightarrow \int_{-\infty}^{-1} h(x) dx + \int_0^1 h(x) dx \\
 &= \int_{-1}^0 h(x) dx + \int_1^{\infty} h(x) dx = \frac{1}{2} \\
 &\Rightarrow \lim_{K \rightarrow \infty} P(K) = \frac{1}{2}.
 \end{aligned}$$

□

3.1.2. The graphs 7₃, 13₃ and 13₈. At this stage we are not able to prove the validity of the conjecture that the nodal sequences resolve the isospectrality of the graphs 7₃, 13₃ and 13₈. However, numerical tests show that for an appreciable fraction of the wavefunctions, the nodal counts are distinct. We shall start the discussion by considering the case 7₃, for which we can turn the counting problem into a geometrical problem.

The vertex wavefunctions which correspond to the same eigenvalues are related by transplantation:

$$\vec{\phi}^{\text{II}} = T\vec{\phi}^{\text{I}}, \quad \vec{\phi}^{\text{I}} = T\vec{\phi}^{\text{II}}, \quad (21)$$

where $\vec{\phi}$ stand now for the vertex wavefunction restricted to the seven interior vertices in these graphs. We have already shown that eigenvectors $\vec{\phi}^{\text{I,II}}$ are either proportional to $\vec{1}$ (the vector with constant entries)- in which case both have a single nodal domain, and $\delta\mu_n = 0$, or the $\vec{\phi}^{\text{I,II}}$ are orthogonal to $\vec{1}$. The six eigenvectors of T^2 with eigenvalue 2 span the orthogonal subspace: three of them correspond to the eigenvalue $+\sqrt{2}$ of T , and the other three correspond to the eigenvalue $-\sqrt{2}$ of T . Any vertex wavefunction $\vec{\phi}^{\text{I}}$, which is not proportional to $\vec{1}$, can be written as

$$\vec{\phi}^{\text{I}} = \cos \alpha |+\rangle + \sin \alpha |-\rangle, \quad (22)$$

where $|\pm\rangle$ stand for arbitrary normalized vectors in the three dimensional subspaces mention above, and $\alpha \in [0, 2\pi]$. Thus,

$$\vec{\phi}^{\text{II}} = T\vec{\phi}^{\text{I}} = \sqrt{2}(\cos \alpha |+\rangle - \sin \alpha |-\rangle) \quad (23)$$

and the difference in nodal numbers comes only through the change of sign of the linear combination. We are not able to make further progress beyond this point, and we shall therefore summarize the numerical findings.

The graph 7₃. Based on the study of approximately 6600 eigenfunctions we find that the difference between the discrete nodal counts can take the values 0, ± 2 only. The nodal counts are different for $\simeq 19\%$ of the wavefunctions.

The graph 13₃. Based on the study of approximately 2000 eigenfunctions we find that the difference between the discrete nodal counts can take the values 0, ± 2 only. The nodal counts are different for $\simeq 22\%$ of the wavefunctions.

The graph 13₈. Based on the study of approximately 4700 eigenfunctions we find that the difference between the discrete nodal counts can take the values 0, ± 2 , ± 4 only. The nodal counts are different for $\simeq 22\%$ of the wavefunctions.

This result is certainly encouraging but not sufficient, and we are trying various options to substantiate it more rigorously.

3.2. The metric nodal sequences

The discussion of the metric nodal sequences is facilitated in the present examples of isospectral graphs since most of them are trees. Then, by making use of Schapotschnikow’s theorem [23], the metric nodal counts $v_n = n$. This applies in particular to the isospectral graphs of the types 7_3 , 13_3 and 13_8 which are tree graphs and $v_n^I = v_n^{II} = n$. The metric counts do not resolve the isospectrality in these cases. However, less trivially connected graphs can be constructed by replacing the basic building block. For such graphs Schapotschnikow’s theorem does not apply, and we expect their metric sequences to be different. Below we shall show that this is true for the pair of dihedral graph where graph II is not a tree.

Consider the pair of dihedral graphs, and let $\{v_n^{I,II}\}$ denote the metric nodal counts of graphs I and II. Using (5) we express the difference $v_n^I - v_n^{II}$ as

$$\delta v_n = v_n^I - v_n^{II} = \frac{1}{2} [1 - \text{sign}(\phi_{2,n}^I \sin(2k_n a)) + \text{sign}(\phi_{2,n}^{II} \sin(2k_n b)) + \text{sign}(\phi_{2,n}^{II} \sin(2k_n c))]. \tag{24}$$

To obtain (24) a slight modification of (5) was needed: the term in the sum that corresponds to a bond with a boundary vertex that has Dirichlet boundary conditions should be modified to be $\lfloor \frac{k_n L_b}{\pi} \rfloor$ instead of $\lfloor \frac{k_n L_b}{\pi} \rfloor + \frac{1}{2} (1 - (-1)^{\lfloor \frac{k_n L_b}{\pi} \rfloor} \text{sign}[\phi_i] \text{sign}[\phi_j])$. In addition while deriving (24) we made use of the identity $\lfloor \frac{2x}{\pi} \rfloor - 2 \lfloor \frac{x}{\pi} \rfloor = \frac{1}{2} (1 - \text{sign}(\sin(2x)))$ and of the freedom to choose the sign of the first component of the wavefunctions to be positive. A theorem by Berkolaiko [24] guarantees that δv_n can only take the values 0 and 1. We would like to compute the distribution of these values on the spectrum. For this purpose we consider the spectral interval $0 < k_n < K$ and study the function

$$Q(x; K) = \frac{1}{N(K)} \#\{n \leq N(K) : \delta v_n = x\} \tag{25}$$

and prove the following theorem.

Theorem 2. Consider the dihedral graphs I, II discussed above with rationally independent bond lengths a, b, c . Then

$$\exists \lim_{K \rightarrow \infty} Q(x, K) = Q(x) \quad \text{and} \quad Q(0) = Q(1) = \frac{1}{2}. \tag{26}$$

Proof of theorem 2. In order to study the $Q(x, K)$ above we consider the distribution of δv_n , which is given by the integral

$$h(x; K) = \langle \delta(x - \delta v_n) \rangle_K = \frac{1}{N(K)} \int_0^K dk \delta(f(a, b, c; k)) \left| \frac{df}{dk} \right| \delta(x - \delta v(a, b, c; k)), \tag{27}$$

where the spectral secular function $f(a, b, c; k)$ is defined in (11) above, and $\delta v(a, b, c; k)$ coincides with δv_n for $k = k_n$ and can be written explicitly as

$$\begin{aligned} \delta v(a, b, c; k) = \frac{1}{2} \left[1 - \text{sign} \left(\cos(2ka) \sin(2ka) + \sin^2(2ka) \left(\cot(2kb) + \cot(2kc) \right. \right. \right. \\ \left. \left. \left. - \frac{1}{\sin(2kb)} - \frac{1}{\sin(2kc)} \right) \right) + \text{sign} \left(\frac{\sin^2(2kb) \sin(2kc)}{\sin(2kb) + \sin(2kc)} \left(\frac{1}{\sin(2ka)} \right. \right. \right. \\ \left. \left. \left. + \cot(2ka) + \cot(2kb) + \cot(2kc) \right) \right) + \text{sign} \left(\frac{\sin(2kb) \sin^2(2kc)}{\sin(2kb) + \sin(2kc)} \right) \right. \\ \left. \times \left(\frac{1}{\sin(2ka)} + \cot(2ka) + \cot(2kb) + \cot(2kc) \right) \right]. \tag{28} \end{aligned}$$

Following the same route as in the proof of theorem (1) we take the limit $K \rightarrow \infty$ while making use of the ergodic theorem, and replace the k integration by an integration over the three torus with coordinates $r = 2ka \bmod 2\pi$, $s = 2kb \bmod 2\pi$ and $t = 2kc \bmod 2\pi$.

$$\begin{aligned} h(x) &= \frac{\pi}{2a + 2b + 2c} \frac{1}{\pi^3} \int_0^{2\pi} dr \int_0^{2\pi} ds \int_0^{2\pi} dt \delta(f(r, s, t)) \left| \frac{df}{dk} \right| \delta(x - \delta v(r, s, t)) \\ &= Q(-1)\delta(x - (-1)) + Q(0)\delta(x) + Q(1)\delta(x - 1) + Q(2)\delta(x - 2). \end{aligned} \quad (29)$$

The last line follows from the fact that x is an integer which is written as half the sum of four unimodular numbers. Next we note that under the transformation $r \mapsto r' = (-r) \bmod 2\pi$, $s \mapsto s' = (-s) \bmod 2\pi$, $t \mapsto t' = (-t) \bmod 2\pi$ we have

$$\begin{aligned} f(r', s', t') &= -f(r, s, t) \\ \frac{df}{dk}(r', s', t') &= \frac{df}{dk}(r, s, t) \\ \delta v(r', s', t') &= 1 - \delta v(r, s, t). \end{aligned}$$

Thus, we conclude that $Q(-1) = Q(2) \wedge Q(0) = Q(1)$. But due to Berkolaiko's theorem [24] $Q(-1) = Q(2) = 0$. Therefore,

$$Q(0) = Q(1) = \frac{1}{2}. \quad \square$$

4. Discussion and summary

There is now a growing amount of evidence that nodal-count sequences store information on the geometry of the system under study, which is similar but not equivalent to the information stored in the spectral sequence. In a recent paper [28] it was shown that the nodal count sequence for separable Laplace–Beltrami operators can be expressed in terms of a trace formula which consists of a smooth (Weyl-like) part, and an oscillatory part. The smooth part depends on constants which can be derived from the geometry of the domain, and the oscillatory part depends on the classical periodic orbits, much in the same way as the spectral trace formula. However, what we have shown in the present paper is that the information stored in the two sequences is not identical: For the isospectral pairs of graphs considered here, the nodal-count sequences are different in a substantial way. In this respect, the nodal sequence resolves isospectrality.

Till this work was done, the conjecture that isospectrality is resolved by counting nodal domains was substantiated by numerical studies only. Here we presented for the first time a system where this fact is proved rigorously. The main breakthrough which enabled the proof was by formulating the counting problem in a geometrical setting. We hope that this way will pave the way to further analytical studies, where more complex systems will be dealt with.

Finally, we would like to mention a set of open problems which naturally arise in the present context: can one find metrically different domains where the Laplacians have different spectra but the nodal counting sequences are the same? A positive answer is provided for domains in one dimension (Sturm) or for tree graphs (Schapotschnikow). Are there other less trivial examples?

Acknowledgments

It is a pleasure to acknowledge S Gnutzmann, M Solomyak and G Berkolaiko for valuable discussions and comments. We are indebted to M Sieber for discussions and for sharing with us his notes which formed the basis for the results discussed in the appendix. The work was

supported by the Minerva Center for non-linear Physics and the Einstein (Minerva) Center at the Weizmann Institute, and by grants from the GIF (grant I-808-228.14/2003), and EPSRC (grant GR/T06872/01. US thanks the School of Mathematics in Bristol for their hospitality and support.

Appendix. Construction of the isospectral dihedral graphs

The Dihedral group D_4 is the symmetry group of a square. Let a be the transformation of rotating the square $\pi/2$ counterclockwise and b be the transformation of reflecting it along the x axis. The Dihedral group is generated by a, b which obey $a^4 = 1, b^2 = 1, bab = a^{-1}$. The eight group elements of D_4 are $\{1, a, a^2, a^3, r_x = b, r_y = aba^{-1}, r_u = ab, r_v = ba\}$. r_x, r_y, r_u, r_v are reflections along the axes x, y, u, v , respectively (figure A1). Note that the multiplication should be read from right to left since the elements are transformations. This group has five irreducible representations (irreps). Four of them are one dimensional and one, which is of our interest, is two dimensional. The two-dimensional representation is

$$\left\{ \begin{array}{l} 1 \mapsto \begin{pmatrix} 1 & 0 \\ 0 & 1 \end{pmatrix}, \quad a \mapsto \begin{pmatrix} 0 & 1 \\ -1 & 0 \end{pmatrix}, \quad a^2 \mapsto \begin{pmatrix} -1 & 0 \\ 0 & -1 \end{pmatrix}, \\ a^3 \mapsto \begin{pmatrix} 0 & -1 \\ 1 & 0 \end{pmatrix}, \quad r_x \mapsto \begin{pmatrix} -1 & 0 \\ 0 & 1 \end{pmatrix}, \quad r_y \mapsto \begin{pmatrix} 1 & 0 \\ 0 & -1 \end{pmatrix}, \\ r_u \mapsto \begin{pmatrix} 0 & 1 \\ 1 & 0 \end{pmatrix}, \quad r_v \mapsto \begin{pmatrix} 0 & -1 \\ -1 & 0 \end{pmatrix} \end{array} \right\}. \quad (\text{A.1})$$

Denote the appropriate basis by which the representation looks as above by $B^I = \{\Psi_1^I, \Psi_2^I\}$. By change of basis using the matrix $T = \frac{1}{\sqrt{2}} \begin{pmatrix} 1 & -1 \\ 1 & 1 \end{pmatrix} (x \mapsto T^{-1}xT)$ we obtain the similar representation

$$\left\{ \begin{array}{l} 1 \mapsto \begin{pmatrix} 1 & 0 \\ 0 & 1 \end{pmatrix}, \quad a \mapsto \begin{pmatrix} 0 & 1 \\ -1 & 0 \end{pmatrix}, \quad a^2 \mapsto \begin{pmatrix} -1 & 0 \\ 0 & -1 \end{pmatrix}, \\ a^3 \mapsto \begin{pmatrix} 0 & -1 \\ 1 & 0 \end{pmatrix}, \quad r_x \mapsto \begin{pmatrix} 0 & 1 \\ 1 & 0 \end{pmatrix}, \quad r_y \mapsto \begin{pmatrix} 0 & -1 \\ -1 & 0 \end{pmatrix}, \\ r_u \mapsto \begin{pmatrix} 1 & 0 \\ 0 & -1 \end{pmatrix}, \quad r_v \mapsto \begin{pmatrix} -1 & 0 \\ 0 & 1 \end{pmatrix} \end{array} \right\}. \quad (\text{A.2})$$

Denote the second basis by $B^{II} = \{\Psi_1^{II}, \Psi_2^{II}\}$. So that $\begin{pmatrix} \Psi_1^{II} \\ \Psi_2^{II} \end{pmatrix} = T \begin{pmatrix} \Psi_1^I \\ \Psi_2^I \end{pmatrix}$. Note that in the first form of the representation r_x and r_y are diagonal and in the second one r_u and r_v are diagonal. This will be exploited soon.

The graph in figure A2(a) obeys the dihedral symmetry. Examine the eigenfunctions of the Schrödinger operator with Neumann boundary conditions on all the vertices. The set of all the eigenfunctions of a certain eigenvalue λ forms a finite-dimensional vector space V with some dimension $\dim V = n$. This vector space is invariant under the action of the dihedral group and therefore V is the carrier space of some representation of D_4 . We are interested in the case that this representation is the two-dimensional irrep of D_4 or that this representation is a reducible representation that contains the two-dimensional irrep. Consider the basis $B^I = \{\Psi_1^I, \Psi_2^I\}$ of this 2D irrep (note that now Ψ_1^I, Ψ_2^I have the meaning of wavefunctions on the graph in figure A2). From the matrix which corresponds to r_x in this basis (see (A.1)) we deduce that Ψ_1^I vanish on the axis x (as an odd function with respect to that axis) and as for

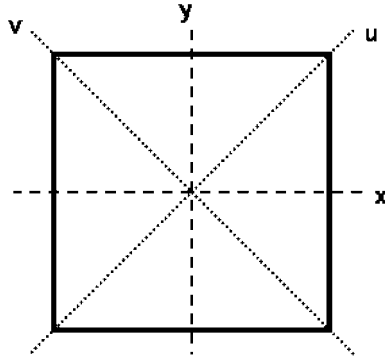


Figure A1. A square with its four possible axes of reflection.

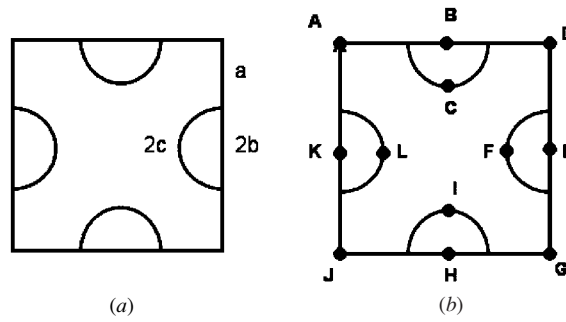


Figure A2. A graph which obeys the dihedral symmetry. In (a) the lengths of the bonds are marked. In (b) The points on which we can deduce boundary conditions are marked.

Ψ_2^I , its derivative vanishes on the x axis (since Ψ_2 is an even function with respect to that axis and therefore its derivative is odd). Using the notation from figure A2(b), we have

$$\Psi_1^I|_{E,F,K,L} = 0 \quad \frac{d}{dx} \Psi_2^I|_{E,F,K,L} = 0. \quad (\text{A.3})$$

Similarly, examining the matrix of r_y in this basis (A.1) yields

$$\frac{d}{dx} \Psi_1^I|_{B,C,I,H} = 0 \quad \Psi_2^I|_{B,C,I,H} = 0. \quad (\text{A.4})$$

We can get similar observations by looking on the matrices of r_u, r_v , this time for the basis $B^{\text{II}} = \{\Psi_1^{\text{II}}, \Psi_2^{\text{II}}\}$ (A.2). We get the following

$$\frac{d}{dx} \Psi_1^{\text{II}}|_{D,J} = 0 \quad \Psi_2^{\text{II}}|_{D,J} = 0 \quad (\text{A.5})$$

$$\Psi_1^{\text{II}}|_{A,G} = 0 \quad \frac{d}{dx} \Psi_2^{\text{II}}|_{A,G} = 0. \quad (\text{A.6})$$

Now, a pair of isospectral graphs will be constructed out of the complete graph. Each of the graphs in the pair will be a subgraph of the complete graph. Graph I is the graph that

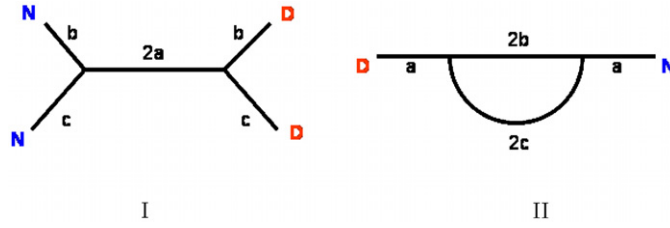


Figure A3. The isospectral pair with boundary conditions. D stands for Dirichlet and N for Neumann.

consists of the vertices B,C,D,E,F and all the bonds which connect them. Graph II is the graph that consists of the vertices A,B,C,D and all the bonds which connect them (figure A3).

We can define the subgraphs in another way which will become convenient later: using the axes x, y, u, v as in figure A1 we define two sets of coordinates (x, y) and (u, v) and use them to examine the complete graph. Graph I is obtained when restricting ourselves to the region $D_I \equiv \{x \geq 0 \wedge y \geq 0\}$ of the complete graph. Graph II is obtained when restricting to the region $D_{II} \equiv \{u \geq 0 \wedge v \geq 0\}$. For a certain eigenvalue λ of the complete graph whose representation contains the 2D irrep discussed before, we can define appropriate eigenfunctions on the two subgraphs by $\psi^I = \Psi_1^I|_{D_I}$, $\psi^{II} = \Psi_1^{II}|_{D_{II}}$. The boundary conditions of ψ^I, ψ^{II} are obtained from (A.3), (A.4), (A.5), (A.6) and are shown in figure A3.

So far we have established the ground for the proof of the following:

Theorem 3. Let σ^I denote the spectra of graph I (with its boundary conditions) and σ^{II} denote the spectra of graph II. Then $\sigma^I \equiv \sigma^{II}$ with account of multiplicities.

Proof of theorem 3. We will make use of the results above in order to construct a transplantation which proves the theorem. Let $\lambda \in \sigma^I$. Denote by V^I the space of eigenfunctions which belong to the eigenvalue λ . $\forall \psi^I \in V^I$ define the functions Ψ_1^I, Ψ_2^I on the complete graph by the following:

$$\Psi_1^I(x, y) = \begin{cases} \psi^I(x, y) & \text{for } x \geq 0 \wedge y \geq 0 \\ -\psi^I(x, -y) & \text{for } x \geq 0 \wedge y \leq 0 \\ \psi^I(-x, y) & \text{for } x \leq 0 \wedge y \geq 0 \\ -\psi^I(-x, -y) & \text{for } x \leq 0 \wedge y \leq 0 \end{cases} \quad (\text{A.7})$$

$$\Psi_2^I(x, y) = -\Psi_1^I(y, -x). \quad (\text{A.8})$$

Where we have used again the coordinates (x, y) as defined trivially by the axes x, y (scaling is obviously not important for our purposes). It can be verified that Ψ_1^I, Ψ_2^I are valid eigenfunctions of the eigenvalue λ defined on the complete graph. If $\Psi_1^I(x, y) = c\Psi_2^I(x, y)$ for some $c \in \mathbb{R}$ then we get that $\psi^I(x, y) = c\psi^I(y, x) \Rightarrow \psi^I \equiv 0$ (this can simply be concluded by considering the boundary conditions). Therefore Ψ_1^I, Ψ_2^I are independent eigenfunctions and form a basis $B^I = \{\Psi_1^I, \Psi_2^I\}$ for the appropriate eigenspace. This is exactly the basis B^I of the first form of the 2D irrep of D_4 (see (A.1)). (This can be verified for example by examining the representation of the generators a, b of D_4). Now, we construct the basis $B^{II} = \{\Psi_1^{II}, \Psi_2^{II}\}$ by $\begin{pmatrix} \Psi_1^{II} \\ \Psi_2^{II} \end{pmatrix} = T \begin{pmatrix} \Psi_1^I \\ \Psi_2^I \end{pmatrix} = \frac{1}{\sqrt{2}} \begin{pmatrix} 1 & -1 \\ 1 & 1 \end{pmatrix} \begin{pmatrix} \Psi_1^I \\ \Psi_2^I \end{pmatrix}$. And now define the function ψ^{II} on graph II by $\psi^{II} = \Psi_1^{II}|_{D_{II}}$. We get that ψ^{II} is an eigenfunction of graph II which belongs to the eigenvalue λ and obeys the appropriate boundary conditions $\Rightarrow \lambda \in \sigma_{II}$.

Following this procedure, one can verify that T is the transplantation matrix of the vertex wavefunctions. We can similarly describe the inverse transplantation. The inverse transplantation is linear and therefore if we have an independent set of eigenfunctions (with the same eigenvalue) they would remain independent after the transplantation. Thus, the degeneracies of λ in σ_I and σ_{II} are equal. The existence of the inverse transplantation also proves that $\forall \lambda \in \sigma_{II} \Rightarrow \lambda \in \sigma_I$ and the degeneracy is again the same. Therefore $\sigma_I \equiv \sigma_{II}$ with account of multiplicities. \square

References

- [1] Gordon C, Webb D and Wolpert S 1992 *Bull. Am. Math. Soc.* **27** 134–8
- [2] Chapman S 1995 *Am. Math. Mon.* **102** 124
- [3] Buser P, Conway J, Doyle P and Semmler K-D 1994 *Int. Math. Res. Not.* **9** 391–400
- [4] Okada Y and Shudo A 2001 *J. Phys. A: Math. Gen.* **34** 5911–22
- [5] Jakobson D, Levitin M, Nadirashvili N and Polterovich I 2006 *J. Comput. Appl. Math.* **194** 141–55
Levitin M, Parnovski L and Polterovich I 2006 *J. Phys. A: Math. Gen.* **39** 2073–82
- [6] Sunada T 1985 *Ann. Math.* **121** 196–86
- [7] Kac M 1966 *Am. Math. Mon.* **73** 1–23
- [8] Milnor J 1964 *Proc. Natl Acad. Sci. USA* **51** 542
- [9] Brüning J 1978 *Math. Z.* **158** 15
- [10] Zelditch S 1998 *J. Differ. Geom.* **49** 207
- [11] Zelditch S 2004 *Surveys in differential geometry* **IX** 401–67
- [12] Fisher M E 1966 *J. Comb. Theory* **1** 105–25
- [13] Gutkin B and Smilansky U 2001 *J. Phys. A.: Math. Gen.* **31** 6061–8
- [14] Brooks R 1999 *Ann. Inst. Fourier* **49** 707–25
- [15] von Below J 2000 *Partial Differential Equations on Multistructures (Lecture Notes in Pure and Applied Mathematics vol 219)* (New York: Dekker) pp 19–36
- [16] Carlson R 1999 *Trans. Am. Math. Soc.* **351** 4069–88
- [17] Blum G, Gnutzmann S and Smilansky U 2002 *Phys. Rev. Lett.* **88** 114101
- [18] Roth J-P *Lectures Notes in Mathematics: Theorie du Potentiel* ed A Dold and B Eckmann (Berlin: Springer) pp 521–39
- [19] Kottos T and Smilansky U 1999 *Ann. Phys., NY* **274** 76
- [20] Gnutzmann S, Smilansky U and Sondergaard N 2005 *J. Phys. A: Math. Gen.* **38** 8921–33
- [21] Shapira Talia and Smilansky Uzy 2004 *Proceedings of the NATO Advanced Research Workshop (Tashkent, Uzbekistan, 2004)* at press
- [22] Gnutzman S, Smilansky U and Weber J 2004 *Waves Random Media* **14** S61–73
- [23] Schapotschnikow P 2006 *Waves Complex Random Media* **16** 167–78
- [24] Berkolaiko G 2006 Private communication
- [25] Davies E B, Leydold J and Stadler P F 2001 *Linear Algebra Appl.* **336** 51
- [26] Barra F and Gaspard P 2000 *J. Stat. Phys.* **101** 283
- [27] Courant R and Hilbert D 1953 *Methods of Mathematical Physics* vol 1 (New York: Interscience) pp 451–65
- [28] Gnutzmann S, Karageorge P D and Smilansky U 2006 *Phys. Rev. Lett.* **97** 090201